Y junctions arising from dark-soliton propagation in photovoltaic media

Minoru Taya

E. L. Ginzton Laboratory, Stanford University, Stanford, California 94305

Matthew C. Bashaw

Department of Electrical Engineering, Stanford University, Stanford, California 94305, and Silicon Valley Photonics, Menlo Park, California 94025

M. M. Fejer

E. L. Ginzton Laboratory, Stanford University, Stanford, California 94305

Mordechai Segev

Department of Electrical Engineering, Center for Photonics and Optoelectronic Materials, Princeton University, Princeton, New Jersey 08544

George C. Valley

Hughes Research Laboratories, Malibu, California 90265

Received December 4, 1995

We report the observation of planar Y-junction waveguide splitters that are due to the bulk photovoltaic effect. The junctions are generated by multiple dark-soliton propagation in $LiNbO_3$ by use of low power levels (20 mW) and average intensities of 10 W/cm^2 at 488 nm. The junctions persist in the dark and can be used to divide input beams of less photorefractive sensitivity. We describe some possibilities for generating other waveguide structures in bulk and thin-film media. © 1996 Optical Society of America

Self-focusing of light that is due to optically induced index perturbations arising in Kerr media[1] has stimulated three decades of investigation of spatial solitons. A bright soliton, in which a beam of light propagates without change in its transverse profile, occurs when self-focusing that is due to a positive light-induced change in the index of refraction balances diffraction. Bright Kerr solitons are inherently unstable in three dimensions[2,3] but can be stable in two dimensions.[4] A dark soliton, in which a dark band, or notch, is superimposed upon an otherwise uniform background illumination, occurs when self-defocusing owing to a negative light-induced index change balances the diffraction of the notch. Although they were predicted some time ago,[5] dark solitons, which require an antisymmetric phase profile, were only recently observed in Kerr media.[6] The recent prediction of bright solitons arising from electric-field-induced carrier drift in photorefractive media[7,8] and the observation of quasi-steady-state bright[9] and dark[10] solitons as well as screening solitons[11] in these media is of interest because of the low light intensities required for self-guiding to be seen. The further prediction of solitons in photovoltaic–photorefractive media[12] and the observation of dark solitons in photovoltaic $LiNbO_3$ (Ref. 13) are significant because external electric fields are not required and the typically long dark lifetime of the charge-induced index perturbations in $LiNbO_3$ permits their use as waveguides long after their initial creation by soliton formation.[13]

The optical nonlinearity responsible for soliton formation in photovoltaic–photorefractive media is due to the transport of an electronic charge, in which photoexcited electrons generate photogalvanic currents proportional to intensity and flowing in the direction of the c axis. This transport results in a space-charge electric field, which, through the electro-optic effect, induces an index perturbation capable of supporting photovoltaic solitons. In, e.g., $LiNbO_3$, the photovoltaic effect results in negative index perturbations, of the order of 10^{-3}–10^{-4}, which are capable of supporting dark solitons. These perturbations are frequently associated with optical degradation in other nonlinear-optical applications[14] and have been used for the formation of volume phase holograms.[15] For open circuit boundary conditions the index perturbation is expected to be proportional to $I/(I + I_{\mathrm{dark}})$, in which I is the intensity and I_{dark} is the dark irradiance equal to the intensity required for a photoconductivity equal to the dark conductivity.[12] The width of planar solitons is expected to vary inversely with the square root of the intensity for intensities smaller than the dark irradiance and to vary approximately with the square root of the intensity for intensities greater than the dark irradiance.[12] Although the features of solitons of on-background beams of finite extent in Kerr media are consistent with those of ideal solitons,[16] observations of photovoltaic solitons on finite background in $LiNbO_3$ have not been fully consistent with the expected intensity dependence and remain a topic of continuing research.[13]

In addition to bright and dark solitons, the latter of which may be black or gray, self-guiding and multisoli-

0146-9592/96/130943-03$10.00/0

tonlike structures may evolve from a variety of input amplitude profiles. These structures include soliton collisions, in which two solitons cross as they propagate through a medium. Dark solitonlike structures typically evolve form dark regions, in a diffraction pattern displaying rapid phase changes that locally approximate odd symmetry.[5,17] Photovoltaic solitons leave behind index perturbations that persist in the dark, and these perturbations can be used to guide beams at wavelengths less sensitive to the photorefractive effect.[13] The selection and generation of an appropriate input amplitude profile permit the generation of multiple interacting solitons. A particularly significant example is the Y junction, in which an appropriate amplitude produces a dark notch that splits into two diverging dark structures. Such structures have been realized in Kerr media.[18]

We report here the observation of planar Y junctions in photovoltaic $LiNbO_3$ whose intensity profiles vary in one transverse dimension. The Y junctions persist in the dark and can be used to distribute a second beam into two waveguides. We form a pair of dark structures by using the experimental arrangement of Fig. 1, which consists of a nominally undoped sample of congruent $LiNbO_3$, a 0.5-mm copper wire, and a telescope to image the collimated beam onto the front crystal surface. All measurements are performed at room temperature. The beam propagates perpendicular to the crystalline c axis. The polarization and the gradient of the planar amplitude profile are parallel to the c axis. Observation of scattered light normal to the direction of propagation allows us to observe the spatial evolution of the incident beam from the side of the crystal. These side views are detected by a CCD array and captured by a computer-controlled frame grabber.

Placing an opaque notch, in this case a strip of wire, on a smoothly varying background beam generates a large number of dark diffraction lines that diverge on propagation. We filter the beam in the central focal plane (Fourier plane) of the telescopic system so that only two diffraction lines remain, and we image the filtered strip onto the front surface of a sample $LiNbO_3$ to produce a narrow dark notch with a full width at half-maximum of $\sim 20\ \mu$m. The power of the notch-bearing beam (of 488-nm wavelength) is 20 mW, with an average intensity of 10 W/cm^2 at the front surface of the crystal. Before formation of the index perturbation the initial notch diffracts into two dark notches that diverge from each other and further diffract into wider notches at the exit surface of the crystal. The side-view profiles in Fig. 2(a) illustrate unperturbed propagation, in which the two dark notches are not easily distinguished. After the refractive-index variation forms (after 30 min), the notches continue to diverge, but each one narrows within the first few millimeters of the medium and maintains a relatively uniform profile through the remainder of the medium; the widths of the trapped dark notches are $\sim 15\ \mu$m, and the divergence angle is ~ 0.5 mrad.

The waveguides associated with the trapped dark notches remain in the absence of illumination and can be probed by a second beam. We introduce a probe beam (of 514-nm wavelength) into the path of the first beam after the wire in Fig. 1 and launch it into the Y junction. The probe beam is of a power comparable with that of the writing beam to generate sufficiently strong scatter profiles. We illuminate the sample for relatively brief time intervals (seconds) to avoid significant erasure of the index perturbation during data acquisition. The structure of the Y junction divides the incident light and directs a significant portion into each of the two waveguides generated by the dark structures, as illustrated in Fig. 2(c).

We can evaluate the data in Fig. 2 quantitatively by examining intensity profiles taken from the images. Because we are imaging coherent volume features in the medium, the profiles represent not an image plane but instead an average of light scattered by the full width of the propagating background beam. The profiles of the initial diffraction pattern corresponding to Fig. 2(a) are shown in Fig. 3(a), illustrating divergence of the two dark structures and significant diffraction of each. The intensity profiles after formation of an index perturbation as in Fig. 2(b) are shown in Fig. 3(b), illustrating continued relative divergence but self-guiding in each dark structure. The profiles of the interaction of a probe beam with the index perturbation, corresponding to Fig. 2(c), are shown in Fig. 3(c), illustrating the division and guiding of the launched beam.

Higher-order fan-in and fan-out structures can be achieved through appropriate spatial filtering. Alter-

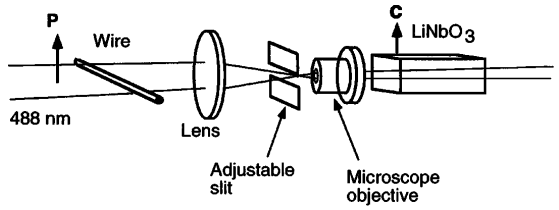

Fig. 1. Experimental arrangement.

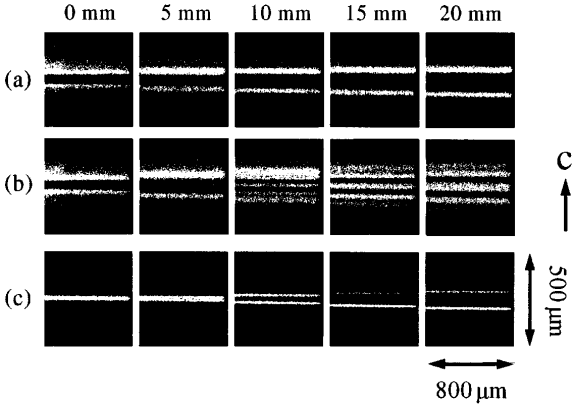

Fig. 2. Properties of an even-amplitude dark profile launched into a 1 cm × 1 cm × 5 cm sample of congruent $LiNbO_3$. The diameter of the background 488-nm beam is ~ 0.6 mm, and the average intensity is ~ 10 W/cm^2. A mosaic of the side view of the 488-nm beam with an intensity step is shown (a) for the initial condition before formation of an index perturbation and (b) after formation of the index perturbation. A corresponding mosaic of the side view of a separate 514-nm beam launched collinearly to the 488-nm beam is shown (c) as it is divided and guided by the Y junction left behind by 488-nm illumination. The images are obtained at 5-mm intervals.

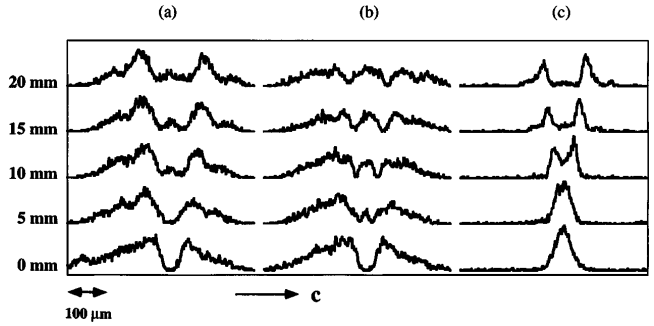

Fig. 3. Profiles of a Y junction launched into a 1 cm × 1 cm × 5 cm sample of congruent $LiNbO_3$. The diameter of the background 488-nm beam is ~0.6 mm, and the average intensity is ~10 W/cm^2. Profiles of the side view of the 488-nm beam with an intensity step are shown (a) for the initial condition before formation of an index perturbation and (b) after formation of the index perturbation. A corresponding mosaic of the side view of a separate 514-nm beam launched collinearly to the 488-nm beam is shown (c) as it is divided and guided by the Y junction left behind left behind by 488-nm illumination. The profiles are obtained at 5-mm intervals.

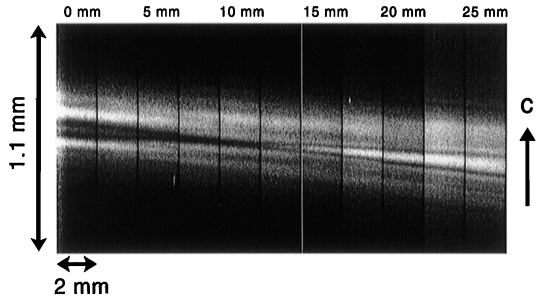

Fig. 4. Side view of an X junction showing complex nonlinear-optical interaction at 488 nm (~3 W/cm^2). The images are obtained at 2.5-mm intervals and show a width of 2 mm.

natively, repositioning of the focusing optics allows dark features to collide within the medium to generate an X junction (Fig. 4). Before steady state, the features are essentially symmetric about the junction, so each dark strip converges and then diverges after collision; after steady state, the dark notches propagate without diffraction but continue to diverge from each other.

We have demonstrated the use of photovoltaic–photorefractive $LiNbO_3$ as a medium in which nontrivial waveguide structures can be generated through nonlinear physical optical means at lower power levels. Two-dimensional transverse confinement can be achieved by generation of similar structures in slab waveguides. The dark decay is expected to be commensurate with the decay time for holograms in $LiNbO_3$, which can be of the order of months to years. The lifetime under illumination is longer at longer wavelengths, but with continuous illumination at most visible wavelengths the index perturbations eventually decay. The index perturbations can be intentionally erased by uniform illumination at the writing wavelength; the erasure rate is proportional to intensity. Fixing techniques such as those used in photorefractive media[19] can be adaptable for use in fixing waveguides generated in this manner. Equally important is the identification of interacting waveguide structures that can be achieved with these techniques and the amplitude profiles required for achieving them.

We are grateful to Y. Furukawa of Hitachi Metals, Ltd., and Crystal Technology, Inc., for growth and preparation of the $LiNbO_3$ samples used in this research. M. Taya, M. Bashaw, and M. Fejer acknowledge support from the Advanced Research Projects Agency and through the Center for Nonlinear Optical Materials at Stanford University. M. Taya acknowledges the support of Shin-Etsu Chemical Co., Ltd. G. Valley acknowledges the support of Hughes Aircraft Company Internal Research and Development.

References

1. R. Y. Chiao, E. Garmire, and C. H. Townes, Phys. Rev. Lett. **13,** 479 (1964).
2. V. E. Zahkarov and A. B. Shabat, Zh. Eksp. Teor. Fiz. **61,** 118 (1971) [Sov. Phys. JETP **34**, 62 (1972)].
3. J. E. Bjorkholm and A. Ashkin, Phys. Rev. Lett. **32,** 129 (1974).
4. A. Barthelomy, S. Maneuf, and C. Froehly, Opt. Commun. **55,** 201 (1985); J. S. Aitchison, A. M. Weiner, Y. Silberberg, M. K. Oliver, J. L. Jackel, D. E. Leaird, E. M. Vogel, and P. W. Smith, Opt. Lett. **15,** 471 (1990).
5. V. E. Zahkarov and A. B. Shabat, Zh. Eksp. Teor. Fiz. **64,** 1627 (1973) [Sov. Phys. JETP **37,** 823 (1973)].
6. G. A. Swartzlander, Jr., D. R. Anderson, J. J. Regan, H. Yin, and A. E. Kaplan, Phys. Rev. Lett. **66,** 1583 (1991); G. R. Allan, S. R. Skinner, D. R. Anderson, and A. L. Smirl, Opt. Lett. **16,** 156 (1991).
7. M. Segev, B. Crosignani, A. Yariv, and B. Fischer, Phys. Rev. Lett. **68,** 923 (1992).
8. M. Segev, G. C. Valley, B. Crosignani, and P. DiPorto, Phys. Rev. Lett. **73,** (1994); D. N. Christodoulides and M. I. Carvalho, J. Opt. Soc. Am. B **12,** 1628 (1995).
9. G. C. Duree, Jr., J. L. Shultz, G. J. Salamo, M. Segev, A. Yariv, B. Crosignani, P. DiPorto, E. J. Sharp, and R. R. Neurgaonkar, Phys. Rev. Lett. **71,** 533 (1993).
10. G. Duree, M. Morin, G. Salamo, M. Segev, B. Crosignani, P. DiPorto, E. Sharp, and A. Yariv, Phys. Rev. Lett. **74,** 1978 (1994).
11. M. F. Shih, M. Segev, G. C. Vallay, G. Salamo, B. Crosignani, and P. DiPorto, Electron. Lett. **31,** 826 (1995).
12. G. C. Valley, M. Segev, B. Crosignani, A. Yariv, M. M. Fejer, and M. C. Bashaw, Phys. Rev. A **50,** R4457 (1994).
13. M. Taya, M. C. Bashaw, M. M. Fejer, M. Segev, and G. C. Valley, Phys. Rev. A **52,** 3095 (1995).
14. A. Ashkin, G. D. Boyd, J. M. Dziedzic, R. G. Smith, A. A. Ballman, J. J. Levenstein, and K. Nassau, Appl. Phys. Lett. **9,** 72 (1966).
15. F. S. Chen, J. T. LaMacchia, and D. B. Fraser, Appl. Phys. Lett. **13,** 223 (1968).
16. Y. S. Kivshar and X. Yang, Opt. Commun. **107,** 93 (1994); W. J. Tomlinson, R. J. Hawkins, A. M. Weiner, J. P. Heritage, and R. N. Thurston, J. Opt. Soc. Am. B **6,** 329 (1989).
17. K. J. Blow, Phys. Lett. A **107,** 55 (1985).
18. B. Luther-Davies and X. Yang, Opt. Lett. **17,** 496 (1992).
19. L. Hesselink and M. C. Bashaw, Opt. Quantum Electron. **25,** S611 (1993); A. S. Kewitsch, A. Yariv, and M. Segev, in *Photorefractive Effects and Materials*, D. D. Nolte, ed. (Kluwer, Norwell, Mass., 1988), pp. 173–219.